International Journal of Thermophysics, Vol. 28, No. 1, February 2007 (© 2007)
DOI: 10.1007/s10765-007-0162-6

Molecular Dynamics Calculation of the Viscosity of Xenon Gas

Raymond D. Mountain[1]

Received December 12, 2006

The density variation of the viscosity of xenon gas is determined using molecular dynamics simulation with a semi-empirical pair potential fit to low-density gas properties. The gas states ranged in density from 0.37 to $7.62\,\mathrm{mol}\cdot\mathrm{dm}^{-3}$, and varied in temperature from 240 $-591\,\mathrm{K}$. The simulation results match the kinetic-theory predictions for the model potential at the lowest density, and systematically lie below the experimental values for higher densities. This indicates the need for many-body interactions to accurately predict the viscosity of xenon gas at even moderate densities. An operational criterion for identifying the density region where kinetic theory is appropriate is proposed.

KEY WORDS: Green-Kubo; molecular dynamics; viscosity; xenon

1. INTRODUCTION

In this note we address the question: What is the proper way to interpret the density dependence of the viscosity of a gas as the density increases? The Rainwater–Friend theory [1–3], provides one answer based on the assumption that atom interactions are pairwise additive. There are two simulation studies of the viscosity of xenon that bear on this question. In the first one, the shear viscosity of xenon at 270 K was determined using a Lennard-Jones potential [4]. The agreement with experiment was good at low density but showed deviations as the density increased. It is not known if the deviations were due to the absence of many-body interactions or due to inadequacy of the model. The second study [5], employed both

[1] Physical and Chemical Properties Division, Chemical Science and Technology Laboratory, National Institute of Standards and Technology, Gaithersburg, Maryland, 20899-8380, U.S.A. E-mail: rmountain@nist.gov

two-body and three-body interactions for dense fluid xenon. Numerically, the Aziz pair potential for xenon employed here [6,7], is very close to the pair potential developed by Barker and coworkers [8], and used in Ref. 5. That study found that three-body interactions were even more important for thermodynamic properties than for the viscosity. Both studies suggest that many-body interactions are important for fluid xenon, but do not provide direct evidence of their importance for the low-density gas. The work presented here directly addresses this question, and shows that a semi-empirical pair potential that accurately reproduces the low-density thermodynamic and transport properties of xenon is not able to accurately generate the density variation of the viscosity of xenon gas over a wider range of temperature and density.

Molecular dynamics simulations are a viable means for estimating the viscosity, η, and thermal conductivity, λ, of gases [4,9]. Here, the equilibrium time correlation function approach, frequently called the Green-Kubo method [10], is used to determine the shear viscosity of xenon gas as functions of temperature and density. The pair potential developed by Aziz and coworkers [6,7], for xenon is used here. This model potential was constructed to reproduce many thermal properties of xenon gas including the shear viscosity. It is a better representation of the xenon pair interaction than current *ab initio* potentials [11]. As expected, the low-density values for the shear viscosity determined using this potential in kinetic-theory calculations [7] closely match the experimental values [12].

The Green-Kubo method determines the viscosity as the time integral of the time correlation function of the off-diagonal elements of the stress tensor. For a system of N particles in a volume V,

$$\eta = \lim_{t\to\infty} \eta(t) = \frac{1}{V k_B T} \int_0^t \langle P_{xy}(s) P_{xy}(0)\rangle ds \tag{1}$$

where k_B is Boltzmann's constant and T is the temperature. The angular brackets indicate an ensemble average of the enclosed quantity. The momentum current P_{xy} is the x-y component of the stress tensor,

$$P_{xy} = \sum_{i=1}^{N} m_i v_i^x v_i^y + \sum_{i\neq j} x_{ij} F_{ij}^y \tag{2}$$

The first sum is the kinetic contribution to the stress, and is the product of the mass and the x- and y-components of the velocity of the particles. The second double sum is the potential contribution, and is the product of the x-component of the separation of a pair of particles and the y-component of the force between the pair. This form is appropriate for pairwise interactions subject to periodic boundary conditions.

In addition to obtaining the density dependence of the viscosity predicted by this potential model, we will clarify some of the issues associated with the use of the Green-Kubo approach when studying low-density fluids. One issue concerns how low a density is required to recover the kinetic-theory result. A related issue is how to adequately sample the correlation function. As the density decreases, the mean time between collisions increases with the result that the integration time needed; to obtain the proper long time limit increases rapidly. Consequently, the length of the simulation needed; to obtain an adequate sample of independent time origins for the time correlation function increases correspondingly rapidly.

2. METHOD

The simulations were performed on systems of 500 atoms placed in a cubic simulation cell with periodic boundary conditions in all three dimensions. The equations of motion for the NVE ensemble were intergrated using the Beeman algorithm [13, 14], with a time step of 10^{-2} ps. The edge of the cell was adjusted so that the desired gas density, was realized. A total of 31 states were examined with temperatures ranging from 240–591 K and densities ranging from 0.37 to 7.62 $\text{mol} \cdot \text{dm}^{-3}$. The density and temperature of the simulated states are listed in Table I in the next section. The kinetic-theory values of the viscosity of xenon [7], match the simulation values at the lowest density examined.

The off-diagonal elements of the stress tensor were generated at each time step, and the current–current time correlation function of those elements was constructed with time origins separated by a time interval of sufficient duration that the time correlation function had effectively decayed to zero before the next time origin was reached. After a considerable amount of testing, it was decided to separate the time origins by 10 ps. A production run produced *fifteen thousand* time origins. Also, the P_{xy}, P_{xz}, and P_{yz} current correlation functions were generated and then averaged at the end of the run.

Even with the large number of time origins used, smoothing of the long time part of the correlation function was required for the time integral to reach a constant value. For long times, the time correlation function fluctuates about zero, and obtaining cancellation of the fluctuations requires a very large number of samples. The smoothing was done by fitting a Gaussian plus an exponential function to the calculated time correlation divided by Vk_BT. The fitting function, $J(t)$, used here is

$$J(t) = a_1 \exp(-(t/\tau_1)^2) + a_2 \exp(-t/\tau_2) \tag{3}$$

Table I. Calculated values of the viscosity of gaseous xenon are listed for the states examined. (Relative differences in the viscosity for two sequential runs, $\Delta\eta/\eta_{ave}$ and τ_2/τ_1 ,the ratio of fitting times, are also listed.)

ρ (mol · dm^{-3})	T (K)	η (μPa · s)	$100\Delta\eta/\eta_{ave}$	τ_2/τ_1
0.37	240	18.5	0	118
	275	22.1	4.5	126
	284	22.1	0.5	125
	303	22.8	2.1	126
	377	28.0	1.1	134
	591	44.2	2.5	153
0.64	275	20.8	6.7	70
	287	22.8	1.3	74
	344	27.1	2.2	75
	378	29.3	1.4	80
1.25	276	22.2	0.4	37
	301	24.5	0	39
	348	28.6	3.5	40
2.03	272	22.8	0.4	25
	303	25.1	5.6	24
	309	25.5	0.4	24
	333	27.3	2.2	24
	365	30.9	0	25
	377	31.0	1.0	25
	433	36.4	6.0	26
	445	36.4	3.0	26
	527	41.7	2.6	27
2.95	281	25.2	1.9	17
	314	27.9	5.4	17
	344	30.3	3.6	17
	405	35.1	7.1	17
	473	39.9	1.0	18
7.62	327	45.9	2.1	6
	378	48.4	1.4	6
	429	53.5	3.0	6
	533	59.7	7.4	6

The initial value of $J(t)$ is the infinite frequency shear modulus of the fluid G_∞ [15]. The Gaussian accurately represents the short-time behavior of the time correlation function in Eq. (1), and the damped exponential describes the long-time behavior. An example of this procedure is shown in Fig. 1, for the state with $T = 473\,K$ and density $= 2.95\,mol \cdot dm^{-3}$. The fitting parameter τ_1 is on the order of 0.2 ps for all of the states examined. The other time parameter, τ_2, varies from about 1 ps for the high-density states to 27 ps for the lowest-density states. The parameter a_1 is

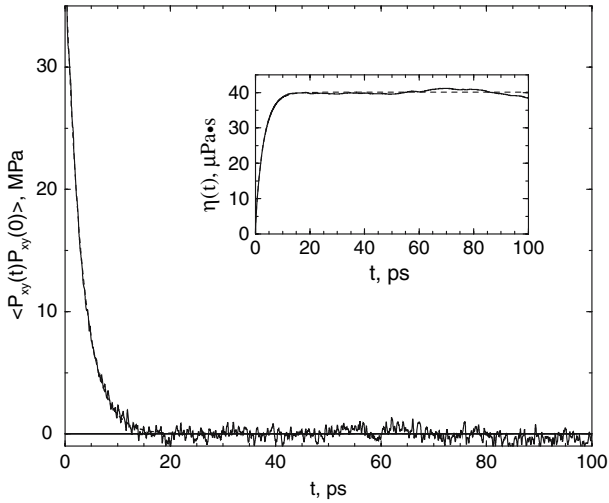

Fig. 1. Time correlation function generated in the simulation is the solid, jagged line, and the Gaussian-exponential fit to the time correlation function is the dashed line. Insert displays $\eta(t)$. Direct integral of the simulation correlation function is the solid line, and the integral of the fit function is the dashed line. For this case, $\tau_1 = 0.17$ ps and $\tau_2 = 3.1$ ps.

an increasing function of density, and a decreasing function of temperature. The parameter a_2 is an increasing function of both density and temperature. This fitting procedure makes sense only if there is a good separation of the fitting times. At higher densities than those considered here, the smoothing function $J(t)$ would not be an appropriate choice. In terms of the fitting parameters, the viscosity is

$$\eta = \frac{a_1 \tau_1}{2} \sqrt{\pi} + a_2 \tau_2 \tag{4}$$

The values of the viscosity reported below were obtained using Eq. (4).

Two methods have been used to estimate the uncertainty in the calculated values of the viscosity. The first is to compare the results for repeated simulations of the same state. This is a very time consuming approach so only two simulations for each of the states were made. In most cases, the absolute value of the difference in the two values of the viscosity was less than 5% of the average of the two values. The distribution of the ratio of the differences to the average value is indicated in Fig. 2. An analysis, of the source of the differences indicates that the intermediate-to-long time variation of the correlation function characterized by τ_2 is the

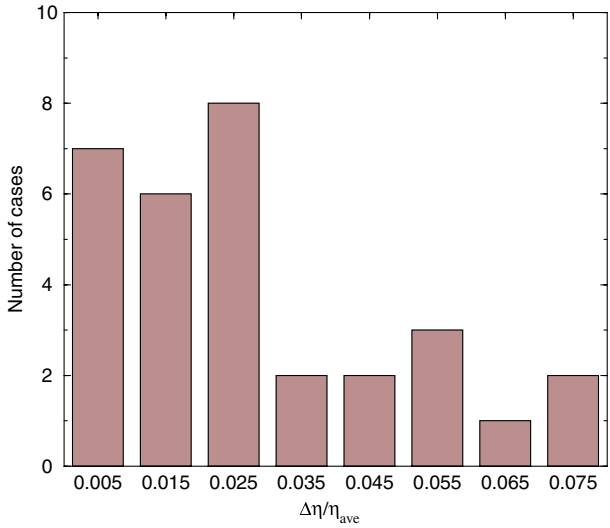

Fig. 2. Ratio of the absolute value of the difference in the calculated values of the viscosity to the average value, $\Delta\eta/\eta_{ave}$, is shown with a resolution of 0.01, for the 31 states of gaseous xenon examined. There is no trend for large differences with either temperature or density.

largest source of the differences. The second approach compared the time correlations for the three individual off-diagonal elements of the stress tensor. Again, most of the cases had estimates that varied by about 5%, or less about the average of the correlation functions for P_{xy}, P_{xz}, and P_{yz}. Again, the largest variation is in the fitting parameter τ_2. The variation from run-to-run is the more conservative estimator in the uncertainty of the viscosity as the difference between two runs are sometimes larger than the difference in the individual component estimated for a single run.

3. RESULTS

The viscosities calculated for the various temperature, and density states are listed in Table I. In Ref. 5 the liquid–vapor phase properties were determined using the Gibbs ensemble method for the pair potential of Barker [8], which is numerically very close to the Aziz potential so we can use those results in determining how close to the coexistence vapor density for this model these states are. This has been confirmed through determinations of the liquid–vapor phase boundary using grand canonical ensemble transition matrix Monte Carlo [16], calculations with the Aziz potential [17]. In all cases, the lowest temperature state examined here lies

well inside the vapor phase. Note that the predicted coexisting vapor densities are significantly lower than the experimental values [18].

In Fig. 3 the viscosities calculated for the lowest density are compared with the kinetic-theory values obtained using the same model potential [7]. As expected, the kinetic-theory values match the measured values extended to zero density [12]. As a rough guide to answering the question of how low a density is needed to recover the kinetic-theory values for a model potential, we note that the ratio of the fitting parameters, a_1/a_2 in Eq. (3), is less than 0.3 for $0.37\,\mathrm{mol}\cdot\mathrm{dm}^{-3}$ states while it is at least 0.5 for $0.64\,\mathrm{mol}\cdot\mathrm{dm}^{-3}$ states. Another measure is the ratio of the time fitting parameters τ_2/τ_1 that are listed in Table I. For the $0.37\,\mathrm{mol}\cdot\mathrm{dm}^{-3}$ states the ratio is 120 or larger while for the $0.64\,\mathrm{mol}\cdot\mathrm{dm}^{-3}$ states, the ratio varies from 70 to 80 as the temperature increases. A separation of the times by about two orders of magnitude seems to be a good indicator of being in the kinetic-theory region. Of course, one should test for density independence, for a given temperature, for a more definitive result. This was done, although not summarized in Table I, and the density of $0.37\,\mathrm{mol}\cdot\mathrm{dm}^{-3}$ was found to be sufficient. The τ_2 times for lower densities

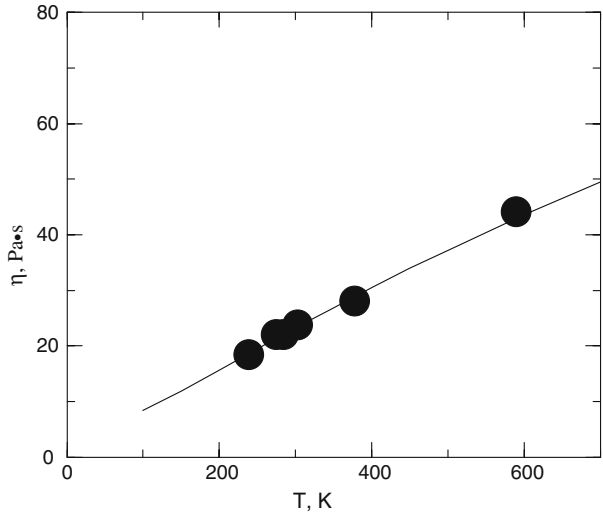

Fig. 3. Kinetic-theory values for the viscosity are shown as the solid line, and the molecular dynamics values of the viscosity on the 0.37 $\mathrm{mol}\cdot\mathrm{dm}^{-3}$ isochore are shown as solid circles. Within the $\pm 5\%$ uncertainty in the molecular dynamics values, the two sets are in good agreement.

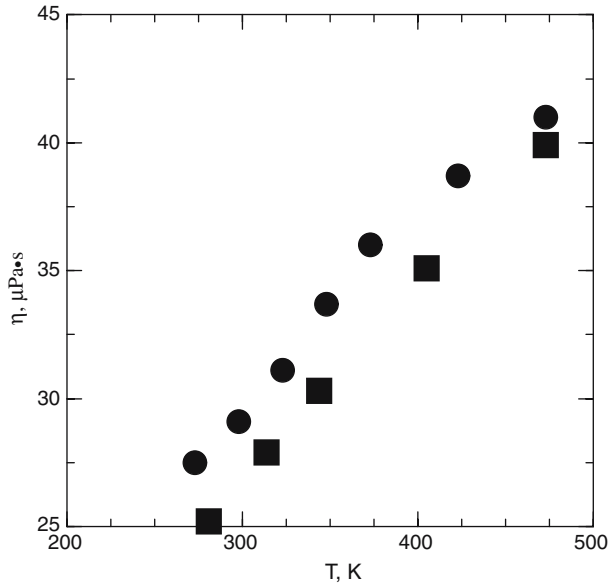

Fig. 4. Calculated values for the viscosity (filled squares), are compared with literature values (solid circles), for the $2.95\,\mathrm{mol}\cdot\mathrm{dm}^{-3}$ isochore. Experimental values for T less than 350 K are from Ref. 20 and those for T greater than 350 K are from Ref. 21.

were quite long, making the determination of a long time value for η(t) less certain.

Next we consider how the computed values of the viscosity at higher densities compares with experimental results. The computed values are systematically lower than the experimental values starting with the $2.03\,\mathrm{mol}\cdot\mathrm{dm}^{-3}$ states. This is illustrated in Fig. 4 for the $2.95\,\mathrm{mol}\cdot\mathrm{dm}^{-3}$ states.

4. DISCUSSION

This paper addresses two issues. The first concerns how low a density is needed to recover the kinetic-theory results. The answer is that the density should be low enough that the time scales represented by the fitting parameters τ_1 and τ_2 should be separated by about two orders of magnitude. The second issue addresses the possible need for including explicit many-body interactions in order to obtain accurate values for the properties of gaseous xenon. The implication of the viscosity calculations is

that higher-order potentials are needed to match the experimental values if an accurate two-body potential is used for xenon. This is consistent with the simulation results for liquid densities [5]. A next step would be to include the triple dipole interactions using the Axilrod–Teller potential [19], as there are indications that other many-body interactions for xenon cancel [5, 11].

The question of how much of the density dependence of the viscosity can be described by the Rainwater–Friend theory [1, 2], and how much requires explict many-body interactions is worth mentioning. The first density-dependent term for the viscosity of the Aziz potential has been determined [3]. Using that result, the simulation values of the viscosity are adequately described for densities up to $1.25\,\mathrm{mol}\cdot\mathrm{dm}^{-3}$. As noted above, the simulation values are systematically less than the experimental values starting with the $2.03\,\mathrm{mol}\cdot\mathrm{dm}^{-3}$ states. This indicates that many-body terms become important for densities on the order of $2\,\mathrm{mol}\cdot\mathrm{dm}^{-3}$ and greater.

REFERENCES

1. D. G. Friend and J. C. Rainwater, *Chem. Phys. Lett.* **107**:590 (1984).
2. J. C. Rainwater and D. G. Friend, *Phys. Rev. A* **36**:4062 (1987).
3. B. Najafi, Y. Ghayeb, J. C. Rainwater, S. Alavi, and R. F. Snider, *Physica A* **260**:31 (1998).
4. G. A. Fernández, J. Vrabec, and H. Hasse, *Fluid Phase Equilibr.* **221**:157 (2004).
5. G. Marcelli, B. D. Todd, and R. J. Sadus, *Fluid Phase Equilibr.* **183**:371 (2001).
6. A. K. Dham, W. J. Meath, A. R. Allnat, R. A. Aziz, and M. J. Salman, *Chem. Phys.* **142**:173 (1990).
7. A. Janzen and R. A. Aziz, *Chem. Eng. Commun.* **135**:161 (1995).
8. J. A. Barker, R. O. Watts, J. K. Lee, T. P. Schafer, and Y. T. Lee, *J. Chem. Phys* **61**:3081 (1974).
9. K. Meier, A. Laesecke, and S. Kabelac, *J. Chem. Phys.* **121**:3671 (2004).
10. J. P. Hansen and I. R. McDonald, *Theory of Simple Liquids*, 2nd Ed. (Academic Press, New York, 1986).
11. A. Malijevský and A. Malijevský, *Molec. Phys.* **101**:3335 (2003).
12. E. Bich, J. Millat, and E. Vogel, *J. Phys. Chem. Ref. Data* **19**:1289 (1990).
13. P. Schofield, *Comput. Phys. Comm.* **5**:17 (1973).
14. D. Beeman, *J. Comput. Phys.* **20**:130 (1976).
15. R. Zwanzig and R. D. Mountain, *J. Chem. Phys.* **43**:4464 (1965).
16. J. R. Errington, *J. Chem. Phys.* **118**:9915 (2003).
17. R. D. Mountain, Unpublished work (2006).
18. O. Šifner and J. Klomfar, *J. Phys. Chem. Ref. Data* **23**:63 (1994).
19. B. M. Axilrod and E. Teller, *J. Chem. Phys.* **11**:299 (1943).
20. N. J. Trappeniers, A. Botzen, C. A. Ten Seldam, H. R. Van Den Berg, and J. Van Oosten, *Physica* **31**:1681 (1965).
21. V. A. Rabinovich, A. A. Vasserman, V. I. Nedostup, and L. S. Veksler, *Thermophysical Properties of Neon, Argon, Krypton and Xenon* (Hemisphere, New York, 1987), pp. 229–230.